JOURNAL OF MATERIALS SCIENCE 32 (1997) 2249–2253

Identification of the morphotropic phase boundary in the lead scandium tantalate–lead titanate solid solution system

J. R. GINIEWICZ, A. S. BHALLA, L. E. CROSS
Materials Research Laboratory, The Pennsylvania State University, University Park, PA 16802, USA

A morphotropic phase boundary between rhombohedral and tetragonal phase regions has been identified to lie in the composition range $x = 0.4$–0.45 by means of X-ray diffraction, and dielectric, pyroelectric, and piezoelectric measurements. Some curvature to this boundary at high temperatures is indicated in the temperature dependences of the dielectric constants and pyroelectric coefficients of poled specimens.

1. Introduction

Several interesting solid solutions of complex lead perovskite compounds and $PbTiO_3$ exist from which materials with enhanced properties and variable behaviour have been generated [1]. These have been shown to be useful systems from both practical and theoretical points of view. Solid-solution systems of rhombohedral lead-based complex perovskites with $PbTiO_3$, generally have so-called "morphotropic phase boundaries" (MPB) that occur between rhombohedral and tetragonal phases at compositions ranging from $x \simeq 0.1$–0.4. It should be noted that the "morphotropic phase boundaries" identified for many of these systems, show some curvature at high temperature and, therefore, strictly speaking, are not truly temperature independent as the name suggests. The boundary between rhombohedral and tetragonal phases is, hence, identified as a MPB in the sense that it is a boundary separating phases whose structure-type depends largely on composition, especially at low temperatures. The compositional "location" of the MPB for a given system has been correlated with the relative stabilities of the tetragonal and rhombohedral phases as predicted by consideration of the perovskite tolerance factor, t [1]. Similar consideration of the $(1-x)\mathrm{Pb}(\mathrm{Sc}_{1/2}\,\mathrm{Ta}_{1/2})\,\mathrm{O}_3 - (x)\mathrm{PbTiO}_3$ system anticipates such a morphotropic phase boundary to occur at $x \approx 0.4$. The actual position of the MPB is most readily assessed by basic structural analysis, in this study conducted by means of X-ray diffraction. Further verification of the compositional range of the boundary and determination of any possible curvature at high temperature may be gained from the temperature variation of numerous material properties across the composition range of interest. In particular, exceptionally strong dielectric, pyroelectric, and piezoelectric responses are typically observed at the MPB of binary systems of this type. The dielectric and pyroelectric responses of poled ceramics are also expected to show features which may be indicative of a curved boundary. The compositional range was initially investigated by means of X-ray diffraction. Verification of these determinations and further insight into the nature of the boundary were gained from subsequent investigation of the dielectric, pyroelectric, and piezoelectric properties of the material through the composition range of the morphotropic phase boundary.

2. Sample preparation

The $(1-x)\mathrm{Pb}(\mathrm{Sc}_{1/2}\,\mathrm{Ta}_{1/2})\mathrm{O}_3$–$(x)\mathrm{PbTiO}_3$ ceramics were produced by a conventional mixed-oxide method involving the use of high-purity starting compounds, a precursor-phase formulation, and controlled lead atmosphere sintering. The compositions of interest were initially prepared as powders employing a wolframite $ScTaO_4$ [2] precursor method [3] in order to reduce the occurrence of undesirable pyrochlore phases. Starting oxides Sc_2O_3 (99.99%, Boulder Scientific Co.) and Ta_2O_5 (standard optical grade, starck, Berlin) were batched and calcined at 1400°C for 6–8 h to form the $ScTaO_4$ precursor. Compositions were then formulated from PbO (Grade A1, Johnson Matthey, Materials Technology, UK), TiO_2 (99.999%, Aesar (Johnson Matthey Inc.)) and the precursor phase across the entire range so as adequately to represent all phase regions occurring in the system. Each composition was calcined at 900 °C for 4 h and at 1000 °C for 1 h with an intermediate comminution step. Compacted specimens of compositions $x \leqslant 0.5$ were fired at 1400 °C for 1 h and those with compositions $x > 0.5$ at 1200 °C also for 1 h within sealed alumina crucibles containing $\mathrm{Pb}(\mathrm{Sc}_{1/2}\,\mathrm{Ta}_{1/2})\mathrm{O}_3/\mathrm{PbZrO}_3$ source powders. Samples with composition $x \geqslant 0.2$ were sufficiently dense ($\approx 95\%$ theoretical density) after this first-stage sintering step; however, specimens with compositions $x \leqslant 0.1$ required a second higher temperature sintering (1500–1560 °C/20 min) which was conducted in

0022–2461 © 1997 Chapman & Hall

a molybdenum tube furnace with a relatively rapid heating and cooling schedule to avoid excessive lead loss. These samples were 90%–95% theoretical density following this second stage sintering step.

The samples prepared for room-temperature X-ray diffraction were all fired under the first-stage sintering conditions and ground to a powder for measurement. Solid specimens were prepared for the high-temperature X-ray diffraction studies. X-ray surfaces were ground with 12 μm Al_2O_3 and the samples were subsequently annealed at 500 °C for 20 min to relieve any surface stresses generated from the grinding.

Specimens for dielectric and pyroelectric measurement were cut as plates from the sintered discs with the dielectric samples typically 0.75 cm on edge and 0.15 cm thick and pyroelectric samples 0.4 cm on edge and 0.025–0.03 cm thick. The specimens for piezoelectric d_{33} coefficient measurement were prepared as blocks typically 0.4 cm on edge and 0.2 cm thick. The electrode surfaces were sputtered with gold to which silver contact points were subsequently applied.

3. Experimental procedure

The structure type, lattice parameters, and theoretical densities were determined for each composition by means of X-ray diffraction using both Philips APD3600 and Scintag (PADV) automated diffractometers. CuK_α radiation was employed. Scans were made on powder samples incorporating a silicon (SRM 640) standard over a range of 42°–52° (2θ) at a rate of 0.25 ° min^{-1} and the 200 and 210 reflections were used to determine the lattice parameters. High-temperature phase transitions were monitored by an X-ray diffraction apparatus designed for use at elevated temperatures extending up to 1000 °C [4].

The dielectric constant, K, and dissipation factor, D, were measured as a function of temperature and frequency using an automated system consisting of an oven (Model 2300, Delta Design, Inc.), an LCR meter (Model 4274A, Hewlett Packard, Inc.), and a digital multimeter interfaced with a desk-top computer (Model 9816, Hewlett Packard, Inc.). Dielectric runs were made at 1 KHz over a temperature range − 150 to 260 °C. The samples were poled in a stirred oil bath at temperatures near the transition temperature under a poling field of 20 kV cm^{-1} for 15 min and then slowly cooled with the field applied to ≈ 50 °C before the poling field was removed.

The pyroelectric response was measured by a modified Byer–Roundy method [5]. The specimens were initially poled in air within a temperature chamber (Model 2300, Delta Design, Inc.) in the vicinity of the transition temperature under a poling field of 20 kV cm^{-1} for 15 min and cooled with the field applied to approximately − 100 °C. The poling field was then removed. A desk-top computer (Model 9816, Hewlett Packard, Inc.) was used to record the pyroelectric current data collected by the picoammeter (Model 4140B, Hewlett Packard, Inc.). The pyroelectric coefficients were subsequently calculated from the pyroelectric current data.

The longitudinal piezoelectric strain coefficient, d_{33}, was determined for specimens, poled as described for the dielectric measurements, utilizing a Berlincourt d_{33} meter (Model CPDT-3300, Channel Products, Inc.). The poled specimens were probed at approximately ten different points and the arithmetic mean of these determinations were recorded as the actual value for a particular sample. The rated accuracy for the Berlincourt meter employed is ± 2% for the range of responses exhibited by these samples.

4. Results and discussion

The structure type, lattice parameter, and theoretical density were determined at room temperature by means of X-ray diffraction for samples extending across the entire compositional range of the system. Complete solid solution is apparent with the morphotropic phase boundary region occurring at $x \approx 0.4$–0.45; the $x \leqslant 0.4$ compositions show a rhombohedral symmetry and compositions $x > 0.4$ possess tetragonal symmetry with a c/a ratio which increases steadily across the tetragonal composition range (Fig. 1; Table I). Samples approaching pure $PbTiO_3$, for which the aspect ratio and, hence, the lattice strains are becoming considerable, like pure $PbTiO_3$, exhibit very low structural integrity. The $x = 0.9$ specimen became fragile and fractured easily within 24 h after sintering. The volume, X-ray density, and aspect ratio, c/a, are given in Table I. An overall decrease in the unit-cell volume and X-ray density is observed.

High-temperature X-ray diffraction revealed the general location of the phase boundary between the high-temperature cubic and lower symmetry phases. The smallest temperature interval practically achieved with this experimental apparatus is approximately 15 °C and, hence, by these means, transition ranges of ≈ 10–20 °C were defined for compositions $x =$ 0.3–0.5 and are recorded in Table I. No evidence of a high-temperature rhombohedral $\rightleftharpoons$ tetragonal transition was detected and, therefore, any significant curvature of the MPB that may exist is assumed, on the basis of these measurements, to occur over a relatively narrow temperature interval in the vicinity of

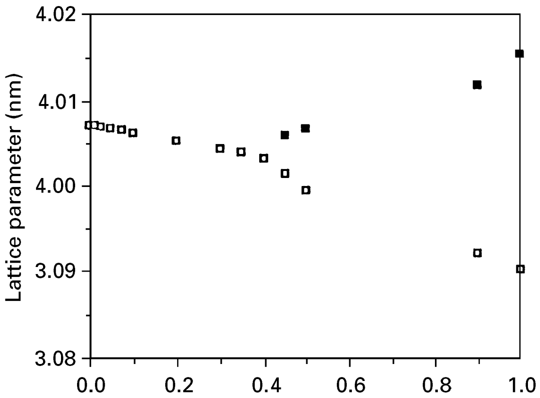

Figure 1 Lattice parameters (25 °C) determined for $(1-x)Pb(Sc_{1/2}Ta_{1/2})O_3$–$(x)PbTiO_3$ ceramics as a function of composition. (□) a, (■) c.

TABLE I Structural data determined by means of X-ray diffraction for various $(1-x)\mathrm{Pb}(\mathrm{Sc}_{1/2}\,\mathrm{Ta}_{1/2})\mathrm{O}_3$–$(x)\mathrm{PbTiO}_3$ compositions

x	Volume (10^{-3}nm^3)	ρ_{XRD} (g cm^{-3})	c/a	Transition range(°C)
0.01	67.53	9.04		
0.025	67.47	9.02		
0.05	67.31	9.00		
0.075	67.29	8.96		
0.1	67.01	8.96		
0.2	66.56	8.86		
0.3	66.10	8.76		150–170
0.35	65.87	8.71		150–170
0.4	65.50	8.67		170–190
0.45	65.39	8.61	1.01	200–220
0.5	64.92	8.58	1.02	220–240
0.9	63.30	8.12	1.05	

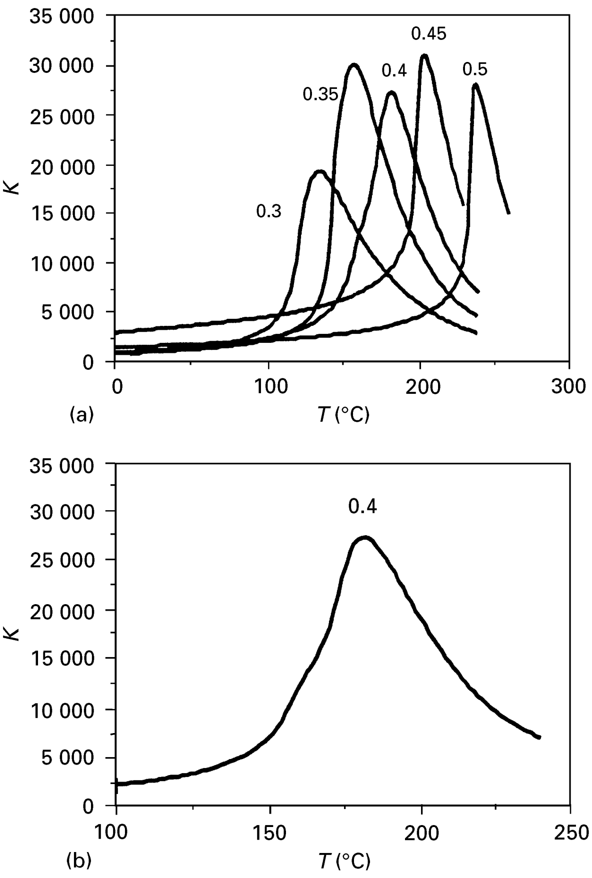

Figure 2 The dielectric constant as a function of temperature at 1 kHz for poled $(1-x)\mathrm{Pb}(\mathrm{Sc}_{1/2}\,\mathrm{Ta}_{1/2})\,\mathrm{O}_3$–$(x)\mathrm{PbTiO}_3$ ceramics: (a) $x = 0.3$–0.5, (b) $x = 0.4$.

the $x = 0.4$ composition. The actual transition temperatures of these compositions were further refined by means of dielectric and pyroelectric property measurements.

The dielectric constant measured at 1 kHz is shown as a function of temperature in Fig. 2a for poled specimens in the composition range $x = 0.3$–0.5. The peak value of $K_{\max}$ is observed for $x = 0.45$. A "shoulder" appears at the low-temperature side of the $x = 0.4$ peak (Fig. 2b) indicative of a possible phase transition preceding the ferroelectric $\rightleftharpoons$ paraelectric transition and, hence, suggestive of some curvature to the MPB at elevated temperatures. It is well-known that the dielectric response, as well as other material properties such as the pyroelectric and piezoelectric responses are particularly enhanced at the MPB of binary systems of this kind and, therefore, the MPB of the $(1-x)\mathrm{Pb}(\mathrm{Sc}_{1/2}\,\mathrm{Ta}_{1/2})\mathrm{O}_3$–$(x)\mathrm{PbTiO}_3$ system may be identified on the basis of these data to be within the composition range $x = 0.4$–0.45, consistent with that determined by means of X-ray diffraction.

The effect of increasing titanium content on the pyroelectric response of the material, as manifested in the temperature dependence of the pyroelectric coefficient, for compositions $x = 0.3$–0.45, is shown in Fig. 3a–d. The change in the shape of $p(T)$ and the magnitudes of the pyroelectric peaks are seen to vary significantly throughout the composition range investigated. A sharp and intense peak is observed for $x = 0.3$ and $x = 0.35$, occurring at temperatures slightly lower than the temperatures of the dielectric constant maxima followed by a doublet at $x = 0.4$ and a somewhat broadened, more intense peak at $x = 0.45$, which also occur at temperatures lower than but increasingly nearer the temperatures of the dielectric constant maxima for these compositions.

A broad high-temperature "hump" has been reported for compositions $x = 0.3$–0.4 from this system [6] which had originally been attributed to a phase transition and, hence, the earlier pyroelectric study identified a broader MPB region with pronounced curvature. It has been determined in this investigation that the currents giving rise to these high-temperature features are apparently non-pyroelectric in nature and more likely some thermally stimulated conduction effect. The marked decrease in the peak pyroelectric response at $x = 0.4$ may well be due to the occurrence of this non-pyroelectric current which would effectively suppress the full pyroelectric response of the material. A more thorough investigation of the conductivity for these compositions is required to determine more accurately the origin and exact nature of this additional component of the induced current.

It is, therefore, assumed at this time that only the sharp lower temperature peaks in this composition range are representative of the actual pyroelectric response of the material and thereby indicative of the phase transitions occurring at each composition. The position and shape of the MPB as defined by these pyroelectric data only are found to be in reasonable agreement with what was determined by means of X-ray diffraction and dielectric measurement.

The magnitudes of the longitudinal piezoelectric strain coefficient, d_{33}, for specimens in the composition range $x = 0.3$–0.5 are recorded in Table II. The maximum longitudinal piezoelectric response is attained for the $x = 0.45$ composition, occurring, as would be expected for a system of this kind, at the morphotropic phase boundary.

5. Conclusion

Room-temperature X-ray diffraction determinations have indicated that complete solid solution occurs across the entire compositional range of the

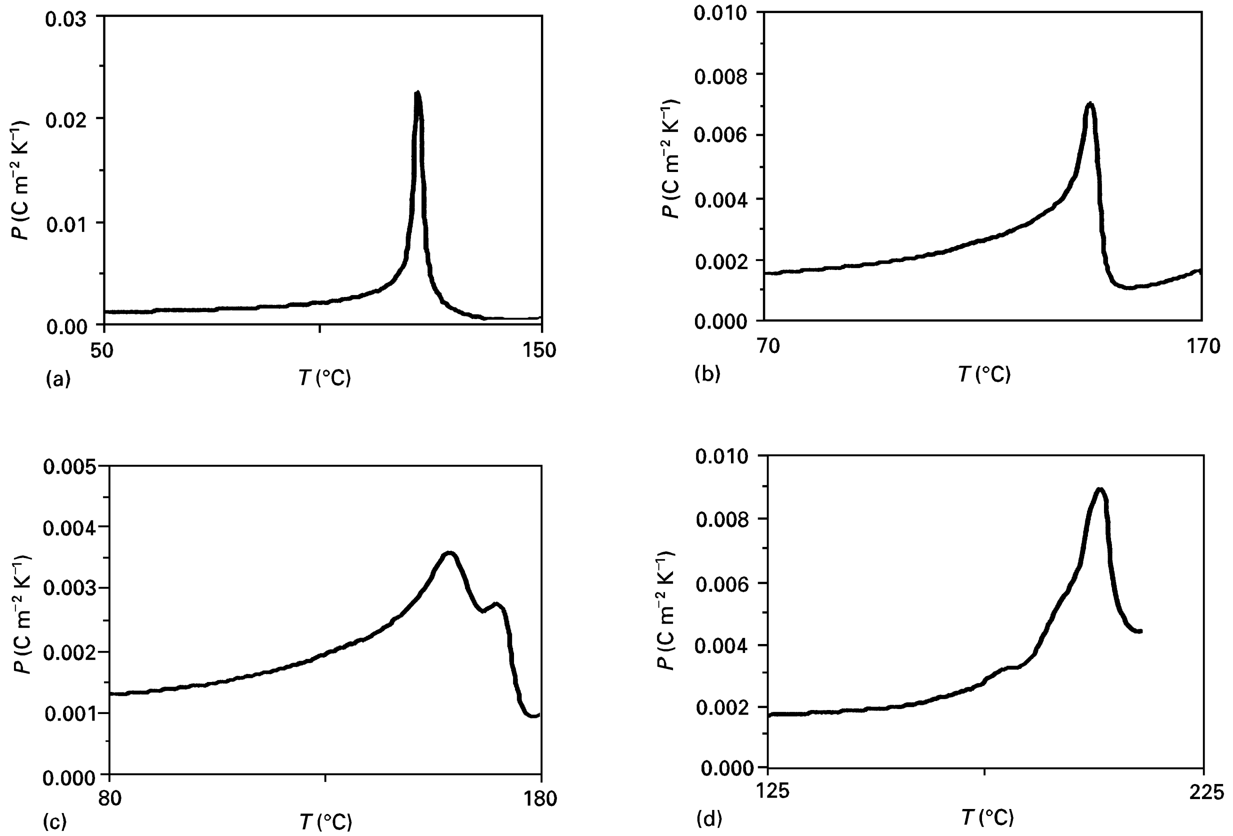

Figure 3 The pyroelectric coefficient as a function of temperature for $(1-x)\mathrm{Pb(Sc_{1/2}\,Ta_{1/2})O_3}$–$(x)\mathrm{PbTiO_3}$ ceramics: (a) $x = 0.3$, (b) $x = 0.35$, (c) $x = 0.4$, and (d) $x = 0.45$.

TABLE II Dielectric, pyroelectric and piezoelectric data for poled $(1-x)\mathrm{Pb(Sc_{1/2}\,Ta_{1/2})O_3}$–$(x)\mathrm{PbTiO_3}$ ceramics in the vicinity of the morphotropic phase boundary

x	$K_{\max}$	T(° C)	$D_{\max}$	T(° C)	$p_{\max}$ (Cm^{-2}K^{-1})	T(° C)	d_{33} (pCN^{-1})
0.3	19 500	135	0.05	124	0.024	123	150
0.35	30 000	160	0.07	154	0.007	145	135
0.4	14 500	162	0.05	175	0.0036	157	180
	27 500	180	–	–	0.0028	170	
0.45	31 000	204	0.05	202	0.095	202	655
0.5	28 200	235	0.03	235	–	–	240

$(1-x)\mathrm{Pb(Sc_{1/2}\,Ta_{1/2})O_3}$–$(x)\mathrm{PbTiO_3}$ system. High-temperature X-ray diffraction studies revealed the general location of the phase boundary between the high-temperature cubic and lower symmetry phases in the composition range $x = 0.3$–0.5 which was further refined by dielectric and pyroelectric measurements.

A morphotropic phase boundary between rhombohedral and tetragonal phase regions was identified by means of X-ray diffraction, dielectric, pyroelectric, and piezoelectric measurements to lie in the composition range $x = 0.4$–0.45. Some curvature to this boundary at high temperatures is indicated in the temperature dependences of the dielectric constants and pyroelectric coefficients of poled specimens.

A summary of the material properties measured in this study for compositions $x = 0.3$–0.5 appear in Table II. The general location of the MPB as defined by the temperatures of the dielectric constant and pyroelectric coefficient maxima of poled specimens is depicted in Fig. 4.

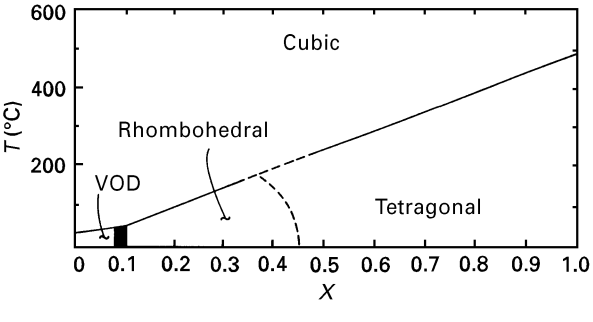

Figure 4 Schematic depiction of the general location of the morphotropic phase boundary as defined by the temperature dependences of the dielectric and pyroelectric responses of poled $(1-x)\mathrm{Pb(Sc_{1/2}\,Ta_{1/2})O_3}$–$(x)\mathrm{PbTiO_3}$ ceramics. VOD-variable order-disorder.

Acknowledgements

The authors thank Dr Chi-Yuen Huang and Dr Herbert McKinstry for collecting the high-temperature X-ray diffraction data for this investigation.

References

1. V. A. ISUPOV, *Bull. Acad. Sci. USSR Phys. Ser.* **47** (1983) 565.
2. JCPDS 24-1017 ($ScTaO_4$) (Joint Committee for Powder Diffraction Studies).
3. T. R. SHROUT and A. HALLIYAL, *Am. Ceram. Soc. Bull.* **66** (1987)704.
4. H. A. MCKINSTRY and H. L. MCKINSTRY, "Computer Interfacing and Programming for a Picker X-Ray Diffractometer/High-Temperature X-Ray Furnace Controller", Pensylvania State University (1984).
5. R. L. BYER and C. B. ROUNDY, *Ferroelectrics* **3**(1972) 333.
6. J. R. GINIEWICZ, A. S. BHALLA, and L. E. CROSS, *Ferroelectrics Lett. Sect.* **12**(2) (1990) 35.

Received 14 June
and accepted 17 September 1996